Supporting Information for

Computational Investigation of Structural Basis for Enhanced Binding of Isoflavone Analogues with Mitochondrial Aldehyde Dehydrogenase

*Yongguang Zhang, Yejie Qiu, and Haiyang Zhang**

Department of Biological Science and Engineering, School of Chemistry and Biological Engineering, University of Science and Technology Beijing, 100083 Beijing, China

Corresponding Author

*zhanghy@ustb.edu.cn

Table S1. Root-Mean-Square Deviation (RMSD, nm) of Monomers (Chain A and Chain B) and the Dimer of ALDH2 Obtained from MD Simulations[a]

compound	chain A	chain B	Dimer
MSA-1	0.17 ± 0.01	0.15 ± 0.01	0.25 ±0.02
OH-1	0.13 ± 0.01	0.12 ± 0.01	0.18 ± 0.01
MSA-2	0.14 ± 0.01	0.13 ± 0.01	0.18 ± 0.01
OH-2	0.17 ± 0.01	0.12 ± 0.01	0.19 ± 0.01
MSA-3	0.18 ± 0.02	0.13 ± 0.01	0.19 ± 0.01
OH-3	0.14 ± 0.01	0.11 ± 0.01	0.16 ± 0.01
MSA-4	0.13 ± 0.01	0.12 ± 0.01	0.15 ± 0.01
OH-4	0.12 ± 0.01	0.14 ± 0.01	0.16 ± 0.01

[a]The last 10 ns trajectories of MD simulations were used for the calculation.

Table S2. Calculated Binding Energies (kJ/mol) of the Inhibitors against ALDH2 by MM-PBSA Using MD-Derived Trajectories as well as the Energy Decomposition[a]

compound	ΔE_{vdW}	ΔE_{elec}	ΔE_{MM}	ΔG_{polar}	$\Delta G_{nonpolar}$	ΔE_{bind}
MSA-1	-258.0 ± 5.1	-64.6 ± 4.7	-322.6 ± 2.1	212.8 ± 6.5	-22.5 ± 0.3	-132.3 ± 7.6
OH-1	-200.5 ± 2.4	-45.8 ± 1.5	-246.3 ± 2.7	138.4 ± 3.7	-17.7 ± 0.2	-125.7 ± 3.7
MSA-2	-233.7 ± 2.2	-45.2 ± 5.6	-278.9 ± 3.9	191.1 ± 10.7	-24.5 ± 0.3	-112.3 ± 7.8
OH-2	-218.9 ± 3.4	-37.0 ± 9.5	-255.9 ± 10.9	165.2 ± 5.2	-22.4 ± 0.4	-113.0 ± 7.0
MSA-3	-243.2 ± 6.2	-64.6 ± 4.7	-307.7 ± 5.3	215.2 ± 5.6	-22.6 ± 0.2	-115.1 ± 4.0
OH-3	-206.5 ± 2.1	-50.7 ± 1.6	-257.2 ± 2.3	169.9 ± 2.5	-18.5 ± 0.3	-105.8 ± 4.7
MSA-4	-222.9 ± 1.8	-64.4 ± 4.0	-287.4 ± 5.4	204.3 ± 6.4	-20.2 ± 0.2	-103.3 ± 3.2
OH-4	-174.7 ± 1.8	-41.6 ± 5.4	-216.3 ± 6.5	144.8 ± 1.9	-16.6 ± 0.2	-88.1 ± 5.6

[a]For each inhibitor, 100 frames from the last 10 ns MD simulations were used for the calculation. ΔE_{MM}, the sum of ΔE_{vdW} and ΔE_{elec}, was calculated in vacuum without cutoff. The energy decomposition in the MM-PBSA analysis refers to eq 1.

Table S3. Contributions from the 4'-Group, 7-Group, and Isoflavone Skeleton of the Inhibitors to the Binding with the Receptor (ALDH2 + NAD^+)[a]

compound	4'-group			7-group			isoflavone skeleton			inhibitor		
	ΔE_{vdW}	ΔE_{ele}	ΔE_{MM}	ΔE_{vdW}	ΔE_{ele}	ΔE_{MM}	ΔE_{vdW}	ΔE_{ele}	ΔE_{MM}	ΔE_{vdW}	ΔE_{ele}	ΔE_{MM}
						receptor (ALDH2 + NAD^+)						
MSA-1	-63.2 ± 2.6	9.6 ± 0.9	-53.6 ± 2.3	-65.7 ± 3.7	16.9 ± 1.7	-48.8 ± 3.6	-129.1 ± 1.1	-91.1 ± 4.3	-220.1 ± 5.1	-258.0 ± 5.1	-64.6 ± 4.7	-322.6 ± 2.1
OH-1	-9.0 ± 1.0	25.0 ± 1.2	15.9 ± 1.0	-45.8 ± 1.2	20.1 ± 1.9	-25.7 ± 2.4	-145.7 ± 0.6	-90.9 ± 1.1	-236.6 ± 1.0	-200.5 ± 2.4	-45.8 ± 1.5	-246.3 ± 2.7
MSA-2	-51.0 ± 0.8	36.3 ± 1.4	-14.7 ± 0.8	-57.3 ± 2.0	22.0 ± 2.9	-35.3 ± 1.6	-125.4 ± 1.1	-103.5 ± 3.3	-228.9 ± 2.1	-233.7 ± 2.2	-45.2 ± 5.6	-278.9 ± 3.9
OH-2	-12.0 ± 0.2	29.6 ± 0.9	17.7 ± 0.9	-71.9 ± 3.0	23.0 ± 9.1	-48.9 ± 10.0	-135.0 ± 1.0	-89.6 ± 0.6	-224.6 ± 1.5	-218.9 ± 3.4	-37.0 ± 9.5	-255.9 ± 10.9
MSA-3	-54.5 ± 2.1	27.6 ± 3.7	-26.9 ± 2.8	-58.3 ± 1.0	20.2 ± 0.8	-38.1 ± 1.4	-130.4 ± 3.4	-112.3 ± 1.6	-242.8 ± 2.8	-243.2 ± 6.2	-64.6 ± 4.7	-307.7 ± 5.3
OH-3	-10.4 ± 0.1	32.0 ± 1.5	21.6 ± 1.5	-53.9 ± 2.2	19.0 ± 1.1	-34.9 ± 1.9	-142.1 ± 1.6	-101.7 ± 1.8	-243.8 ± 3.0	-206.5 ± 2.1	-50.7 ± 1.6	-257.2 ± 2.3
MSA-4	-50.9 ± 1.6	20.0 ± 4.7	-30.9 ± 5.8	-31.8 ± 0.8	28.2 ± 2.2	-3.6 ± 1.5	-140.3 ± 0.6	-112.6 ± 2.8	-252.9 ± 3.1	-222.9 ± 1.8	-64.4 ± 4.0	-287.4 ± 5.4
OH-4	-9.4 ± 1.2	29.5 ± 2.5	20.1 ± 1.8	-27.5 ± 1.5	29.6 ± 3.3	2.0 ± 2.5	-137.7 ± 2.5	-100.7 ± 2.8	-238.4 ± 5.0	-174.7 ± 1.8	-41.6 ± 5.4	-216.3 ± 6.5
						ALDH2						
MSA-1	-56.3 ± 2.0	9.8 ± 1.3	-46.5 ± 1.6	-65.7 ± 3.7	13.7 ± 1.6	-51.9 ± 3.7	-126.6 ± 1.2	-78.6 ± 4.3	-205.2 ± 5.1	-248.5 ± 4.8	-55.1 ± 5.1	-303.6 ± 2.5
OH-1	-9.3 ± 0.2	29.7 ± 0.8	20.4 ± 0.9	-45.8 ± 1.2	17.9 ± 1.9	-27.9 ± 2.4	-140.1 ± 0.7	-82.2 ± 1.1	-222.3 ± 0.8	-195.1 ± 1.4	-34.7 ± 1.2	-229.8 ± 2.4
MSA-2	-46.4 ± 0.8	29.9 ± 1.7	-16.5 ± 1.1	-57.2 ± 2.0	18.5 ± 2.9	-38.8 ± 1.6	-124.9 ± 1.2	-93.1 ± 3.1	-218.0 ± 2.0	-228.6 ± 2.3	-44.7 ± 5.5	-273.3 ± 3.9
OH-2	-10.7 ± 0.2	26.4 ± 0.8	15.7 ± 0.7	-71.9 ± 3.0	20.3 ± 9.0	-51.6 ± 9.9	-130.5 ± 0.9	-83.0 ± 0.8	-213.4 ± 1.3	-213.1 ± 3.2	-36.2 ± 9.4	-249.3 ± 10.5
MSA-3	-49.3 ± 1.1	22.6 ± 2.5	-26.7 ± 2.6	-58.3 ± 1.0	17.0 ± 0.8	-41.3 ± 1.4	-129.9 ± 3.4	-101.8 ± 1.8	-231.6 ± 3.0	-237.5 ± 4.7	-62.2 ± 3.2	-299.7 ± 6.0
OH-3	-9.8 ± 0.2	27.4 ± 1.3	17.6 ± 1.4	-53.9 ± 2.2	14.8 ± 1.0	-39.1 ± 1.8	-140.3 ± 1.6	-91.6 ± 1.6	-231.8 ± 2.9	-204.0 ± 2.0	-49.4 ± 1.8	-253.4 ± 2.1
MSA-4	-49.1 ± 1.8	14.5 ± 4.9	-34.6 ± 6.0	-31.7 ± 0.8	24.7 ± 2.3	-7.0 ± 1.6	-138.4 ± 0.5	-102.5 ± 2.7	-240.9 ± 2.8	-219.2 ± 1.5	-63.3 ± 3.9	-282.5 ± 4.8
OH-4	-8.9 ± 1.3	24.8 ± 2.6	15.9 ± 1.8	-27.5 ± 1.5	25.6 ± 3.3	-1.9 ± 2.5	-136.5 ± 2.4	-90.7 ± 2.7	-227.2 ± 4.8	-172.9 ± 1.7	-40.3 ± 5.4	-213.2 ± 6.3
						NAD^+						
MSA-1	-6.9 ± 0.8	-0.2 ± 0.5	-7.1 ± 1.2	0.0 ± 0.0	3.1 ± 0.2	3.1 ± 0.2	-2.5 ± 0.2	-12.4 ± 0.3	-14.9 ± 0.4	-9.5 ± 0.7	-9.5 ± 0.4	-19.0 ± 0.9
OH-1	0.3 ± 1.2	-4.7 ± 1.1	-4.5 ± 0.4	0.0 ± 0.0	2.3 ± 0.1	2.2 ± 0.1	-5.6 ± 0.3	-8.6 ± 0.3	-14.2 ± 0.4	-5.4 ± 1.1	-11.1 ± 1.2	-16.5 ± 0.7
MSA-2	-4.6 ± 0.4	6.4 ± 0.4	1.9 ± 0.6	0.0 ± 0.0	3.5 ± 0.1	3.5 ± 0.1	-0.5 ± 0.1	-10.4 ± 0.2	-10.9 ± 0.2	-5.1 ± 0.5	-0.5 ± 0.5	-5.6 ± 0.7
OH-2	-1.2 ± 0.1	3.2 ± 0.4	1.9 ± 0.4	0.0 ± 0.0	2.7 ± 0.1	2.7 ± 0.1	-4.5 ± 0.3	-6.6 ± 0.4	-11.2 ± 0.2	-5.8 ± 0.3	-0.7 ± 0.2	-6.5 ± 0.4

MSA-3	-5.1 ± 1.7	4.9 ± 3.2	-0.2 ± 2.2	0.0 ± 0.0	3.3 ± 0.0	3.2 ± 0.0	-0.5 ± 0.0	-10.6 ± 0.3	-11.1 ± 0.3	-5.7 ± 1.7	-2.4 ± 3.2	-8.1 ± 2.1
OH-3	-0.6 ± 0.0	4.6 ± 0.5	4.0 ± 0.4	0.0 ± 0.0	4.2 ± 0.1	4.2 ± 0.1	-1.9 ± 0.1	-10.1 ± 0.2	-12.0 ± 0.3	-2.5 ± 0.2	-1.3 ± 0.4	-3.8 ± 0.4
MSA-4	-1.8 ± 0.3	5.5 ± 1.3	3.7 ± 1.6	0.0 ± 0.0	3.5 ± 0.1	3.5 ± 0.1	-1.9 ± 0.4	-10.1 ± 0.2	-12.1 ± 0.4	-3.7 ± 0.7	-1.1 ± 1.4	-4.8 ± 2.0
OH-4	-0.5 ± 0.1	4.7 ± 0.1	4.1 ± 0.1	0.0 ± 0.0	4.0 ± 0.0	4.0 ± 0.0	-1.2 ± 0.2	-10.0 ± 0.1	-11.2 ± 0.3	-1.8 ± 0.2	-1.3 ± 0.2	-3.1 ± 0.3

[a]Electrostatic and vdW interactions and the sum of both interactions (ΔE_{MM}) are given to evaluate the effect of changing groups on the binding. The inhibitor is divided into three fragments of 4'-group, 7-group, and the isoflavone skeleton. The cofactor NAD^+ is regarded as a residue of the receptor.

Table S4. Energy Decomposition (kJ/mol) for the Key Residues with a Large Contribution to the Receptor–Inhibitor Binding[a]

residue	ΔE_{MM}	ΔE_{polar}	$\Delta E_{nonpolar}$	ΔE_{bind}	Residue	ΔE_{MM}	ΔE_{polar}	$\Delta E_{nonpolar}$	ΔE_{bind}
		MSA-1					OH-1		
VAL120	-5.3 ± 0.1	-0.3 ± 0.1	-0.8 ± 0.0	-6.4 ± 0.1	VAL120	-6.0 ± 0.2	0.0 ± 0.0	-0.9 ± 0.0	-6.8 ± 0.2
ASP121	-1.3 ± 0.1	-0.7 ± 0.2	0.0 ± 0.0	-2.0 ± 0.2	ASP121	-1.5 ± 0.1	-0.3 ± 0.2	0.0 ± 0.0	-1.8 ± 0.2
ASP123	0.3 ± 0.2	-2.7 ± 0.2	0.0 ± 0.0	-2.4 ± 0.2	ASP123	1.2 ± 0.2	-1.8 ± 0.2	-0.0 ± 0.0	-0.6 ± 0.2
MET124	-6.6 ± 0.2	2.0 ± 0.1	-0.7 ± 0.0	-5.3 ± 0.1	MET124	-3.6 ± 0.1	1.6 ± 0.1	-0.4 ± 0.0	-2.3 ± 0.1
LYS127	-2.1 ± 0.3	9.0 ± 0.7	-0.1 ± 0.0	6.8 ± 0.5	LYS127	-1.8 ± 0.2	2.1 ± 0.2	-0.0 ± 0.0	0.3 ± 0.1
PHE170	-10.0 ± 0.1	2.2 ± 0.0	-0.6 ± 0.0	-8.5 ± 0.1	PHE170	-12.6 ± 0.1	2.5 ± 0.0	-0.6 ± 0.0	-10.8 ± 0.2
MET174	-5.4 ± 0.1	3.5 ± 0.1	-0.4 ± 0.0	-2.3 ± 0.1	MET174	-3.4 ± 0.1	2.7 ± 0.1	-0.2 ± 0.0	-0.9 ± 0.1
TRP177	-4.9 ± 0.1	1.6 ± 0.1	-0.2 ± 0.0	-3.5 ± 0.1	TRP177	-6.9 ± 0.1	2.0 ± 0.0	-0.4 ± 0.0	-5.3 ± 0.1
LYS178	2.9 ± 0.0	-5.5 ± 0.2	0.0 ± 0.0	-2.6 ± 0.2	LYS178	-0.7 ± 0.1	0.5 ± 0.1	0.0 ± 0.0	-0.2 ± 0.1
GLU268	-12.3 ± 0.1	13.9 ± 0.4	-0.2 ± 0.0	1.5 ± 0.3	GLU268	-0.2 ± 0.0	-0.7 ± 0.1	-0.0 ± 0.0	-0.9 ± 0.1
GLU288	-0.8 ± 0.0	0.0 ± 0.0	0.0 ± 0.0	-0.7 ± 0.0	GLU288	-1.0 ± 0.1	-0.1 ± 0.1	0.0 ± 0.0	-1.1 ± 0.1
PHE292	-0.4 ± 0.0	0.1 ± 0.0	0.0 ± 0.0	-0.2 ± 0.0	PHE292	-3.1 ± 0.1	1.4 ± 0.1	-0.6 ± 0.0	-2.3 ± 0.1
PHE296	-6.7 ± 0.2	1.4 ± 0.0	-0.6 ± 0.0	-5.9 ± 0.2	PHE296	-8.1 ± 0.1	1.7 ± 0.0	-0.5 ± 0.0	-6.9 ± 0.1
ASP457	-15.0 ± 0.2	22.8 ± 0.4	-1.1 ± 0.0	6.7 ± 0.4	ASP457	-15.5 ± 0.3	25.1 ± 0.7	-0.8 ± 0.0	8.8 ± 0.6
PHE459	-16.2 ± 0.3	4.8 ± 0.1	-1.1 ± 0.0	-12.6 ± 0.2	PHE459	-11.8 ± 0.1	1.8 ± 0.0	-0.7 ± 0.0	-10.7 ± 0.1
GLU476	-2.3 ± 0.0	2.6 ± 0.1	0.0 ± 0.0	0.3 ± 0.1	GLU476	-0.1 ± 0.1	-0.1 ± 0.1	0.0 ± 0.0	-0.2 ± 0.1
NAD^+	-9.5 ± 0.2	12.4 ± 0.2	-0.3 ± 0.0	2.6 ± 0.2	NAD+	-8.3 ± 0.2	10.1 ± 0.2	-0.1 ± 0.0	1.8 ± 0.2
		MSA-2					OH-2		
VAL120	-6.8 ± 0.1	-0.2 ± 0.0	-1.1 ± 0.0	-8.0 ± 0.1	VAL120	-6.5 ± 0.1	0.2 ± 0.0	-0.8 ± 0.0	-7.2 ± 0.1
ASP121	-0.5 ± 0.1	-3.7 ± 0.3	0.0 ± 0.0	-4.2 ± 0.3	ASP121	-1.0 ± 0.1	-2.6 ± 0.1	0.0 ± 0.0	-3.6 ± 0.2
ASP123	-2.4 ± 0.1	-2.8 ± 0.1	-0.0 ± 0.0	-5.2 ± 0.1	ASP123	-1.3 ± 0.1	-1.4 ± 0.1	0.0 ± 0.0	-2.7 ± 0.1
MET124	-3.5 ± 0.1	0.8 ± 0.1	-0.3 ± 0.0	-3.0 ± 0.1	MET124	-3.5 ± 0.1	1.7 ± 0.1	-0.3 ± 0.0	-2.1 ± 0.1

LYS127	2.2 ± 0.1	2.1 ± 0.1	0.0 ± 0.0	4.3 ± 0.1	LYS127	1.1 ± 0.1	1.2 ± 0.1	0.0 ± 0.0	2.3 ± 0.1
PHE170	-7.2 ± 0.1	2.2 ± 0.0	-0.5 ± 0.0	-5.5 ± 0.1	PHE170	-9.4 ± 0.1	2.3 ± 0.0	-0.5 ± 0.0	-7.6 ± 0.1
MET174	-6.1 ± 0.1	3.9 ± 0.1	-0.5 ± 0.0	-2.7 ± 0.1	MET174	-5.8 ± 0.2	2.4 ± 0.1	-0.6 ± 0.0	-4.0 ± 0.2
TRP177	-4.8 ± 0.1	1.8 ± 0.0	-0.3 ± 0.0	-3.3 ± 0.1	TRP177	-7.9 ± 0.1	3.0 ± 0.1	-0.6 ± 0.0	-5.5 ± 0.1
LYS178	3.7 ± 0.1	-5.2 ± 0.3	-0.0 ± 0.0	-1.6 ± 0.2	LYS178	2.8 ± 0.1	-6.5 ± 0.2	-0.0 ± 0.0	-3.7 ± 0.2
GLU268	-8.9 ± 0.3	21.2 ± 1.3	-0.4 ± 0.0	11.9 ± 1.2	GLU268	-3.9 ± 0.1	10.9 ± 0.4	-0.1 ± 0.0	6.9 ± 0.4
GLU288	-5.8 ± 0.2	0.7 ± 0.3	-0.4 ± 0.0	-5.5 ± 0.3	GLU288	-2.7 ± 0.4	-0.4 ± 0.4	-0.0 ± 0.0	-3.0 ± 0.2
PHE292	-9.6 ± 0.2	1.9 ± 0.1	-1.3 ± 0.0	-9.0 ± 0.2	PHE292	-5.4 ± 0.2	1.7 ± 0.1	-1.0 ± 0.0	-4.6 ± 0.2
PHE296	-6.5 ± 0.1	1.8 ± 0.0	-0.6 ± 0.0	-5.2 ± 0.1	PHE296	-7.4 ± 0.2	2.1 ± 0.0	-0.5 ± 0.0	-5.8 ± 0.2
ASP457	-7.6 ± 0.3	19.5 ± 0.6	-1.0 ± 0.0	10.8 ± 0.6	ASP457	-10.7 ± 0.2	23.5 ± 0.6	-0.8 ± 0.0	12.0 ± 0.6
PHE459	-12.9 ± 0.2	2.0 ± 0.0	-0.8 ± 0.0	-11.6 ± 0.2	PHE459	-13.2 ± 0.2	2.5 ± 0.0	-0.8 ± 0.0	-11.6 ± 0.2
GLU476	-2.5 ± 0.1	2.6 ± 0.1	-0.0 ± 0.0	0.0 ± 0.1	GLU476	-4.8 ± 0.1	10.7 ± 0.4	-0.1 ± 0.0	5.8 ± 0.4
NAD^+	-2.8 ± 0.1	7.4 ± 0.1	-0.3 ± 0.0	4.4 ± 0.2	NAD^+	-3.2 ± 0.0	8.6 ± 0.1	-0.1 ± 0.0	5.3 ± 0.1
		MSA-3					OH-3		
VAL120	-6.7 ± 0.1	0.6 ± 0.1	-0.9 ± 0.0	-6.9 ± 0.1	VAL120	-6.6 ± 0.1	-0.1 ± 0.0	-0.7 ± 0.0	-7.4 ± 0.1
ASP121	-5.3 ± 0.2	0.4 ± 0.2	0.0 ± 0.0	-4.9 ± 0.2	ASP121	-1.0 ± 0.1	-2.5 ± 0.1	0.0 ± 0.0	-3.4 ± 0.1
ASP123	-2.7 ± 0.2	1.2 ± 0.4	-0.1 ± 0.0	-1.6 ± 0.2	ASP123	-0.3 ± 0.2	-2.7 ± 0.1	0.0 ± 0.0	-3.0 ± 0.1
MET124	-8.2 ± 0.1	3.2 ± 0.0	-0.7 ± 0.0	-5.7 ± 0.1	MET124	-6.1 ± 0.2	2.5 ± 0.1	-0.6 ± 0.0	-4.3 ± 0.1
LYS127	0.2 ± 0.2	4.3 ± 0.3	-0.1 ± 0.0	4.4 ± 0.3	LYS127	-0.2 ± 0.2	2.4 ± 0.1	0.0 ± 0.0	2.2 ± 0.1
PHE170	-13.8 ± 0.2	3.6 ± 0.0	-1.0 ± 0.0	-11.2 ± 0.2	PHE170	-9.1 ± 0.1	2.2 ± 0.0	-0.5 ± 0.0	-7.4 ± 0.1
MET174	-7.7 ± 0.2	3.1 ± 0.1	-0.4 ± 0.0	-5.0 ± 0.2	MET174	-5.6 ± 0.1	3.3 ± 0.1	-0.4 ± 0.0	-2.7 ± 0.1
TRP177	-7.3 ± 0.1	2.2 ± 0.1	-0.4 ± 0.0	-5.6 ± 0.1	TRP177	-7.8 ± 0.2	3.5 ± 0.1	-0.6 ± 0.0	-4.9 ± 0.2
LYS178	3.5 ± 0.2	-4.5 ± 0.2	-0.0 ± 0.0	-1.0 ± 0.1	LYS178	-0.0 ± 0.2	0.7 ± 0.3	-0.0 ± 0.0	0.6 ± 0.3
GLU268	-6.7 ± 0.4	11.1 ± 0.8	-0.1 ± 0.0	4.3 ± 0.5	GLU268	-0.4 ± 0.2	6.3 ± 0.5	-0.1 ± 0.0	5.8 ± 0.5
GLU288	-0.4 ± 0.1	-0.2 ± 0.0	0.0 ± 0.0	-0.6 ± 0.1	GLU288	-0.3 ± 0.1	-0.5 ± 0.0	0.0 ± 0.0	-0.8 ± 0.1
PHE292	-0.4 ± 0.0	-0.0 ± 0.0	-0.0 ± 0.0	-0.5 ± 0.0	PHE292	-5.4 ± 0.1	0.9 ± 0.0	-0.7 ± 0.0	-5.2 ± 0.1

PHE296	-7.2 ± 0.1	1.4 ± 0.0	-0.8 ± 0.0	-6.5 ± 0.1	PHE296	-6.4 ± 0.1	1.1 ± 0.0	-0.4 ± 0.0	-5.7 ± 0.1
ASP457	-18.2 ± 0.3	22.4 ± 0.5	-1.2 ± 0.0	3.0 ± 0.4	ASP457	-18.9 ± 0.2	32.4 ± 0.4	-0.6 ± 0.0	12.9 ± 0.5
PHE459	-18.7 ± 0.2	5.2 ± 0.1	-1.3 ± 0.0	-14.7 ± 0.2	PHE459	-14.7 ± 0.2	2.9 ± 0.1	-0.7 ± 0.0	-12.5 ± 0.2
GLU476	-2.1 ± 0.1	2.2 ± 0.1	0.0 ± 0.0	0.1 ± 0.1	GLU476	-0.6 ± 0.1	-0.3 ± 0.1	-0.0 ± 0.0	-0.9 ± 0.1
NAD^+	-4.1 ± 0.2	7.7 ± 0.2	-0.2 ± 0.0	3.4 ± 0.2	NAD^+	-1.9 ± 0.1	3.6 ± 0.1	-0.0 ± 0.0	1.7 ± 0.1
		MSA-4					OH-4		
VAL120	-4.9 ± 0.1	-0.4 ± 0.0	-0.6 ± 0.0	-5.9 ± 0.1	VAL120	-4.1 ± 0.1	0.0 ± 0.0	-0.5 ± 0.0	-4.6 ± 0.1
ASP121	0.0 ± 0.1	-2.0 ± 0.2	0.0 ± 0.0	-1.9 ± 0.2	ASP121	-1.2 ± 0.1	-2.1 ± 0.2	-0.0 ± 0.0	-3.4 ± 0.1
ASP123	1.3 ± 0.1	-2.0 ± 0.1	0.0 ± 0.0	-0.7 ± 0.1	ASP123	-1.4 ± 0.1	-1.1 ± 0.1	-0.0 ± 0.0	-2.5 ± 0.1
MET124	-3.5 ± 0.2	1.7 ± 0.1	-0.3 ± 0.0	-2.2 ± 0.1	MET124	-4.6 ± 0.1	2.0 ± 0.1	-0.5 ± 0.0	-3.1 ± 0.1
LYS127	-1.0 ± 0.1	1.5 ± 0.1	0.0 ± 0.0	0.5 ± 0.1	LYS127	1.0 ± 0.1	1.2 ± 0.1	0.0 ± 0.0	2.1 ± 0.1
PHE170	-9.2 ± 0.2	2.0 ± 0.0	-0.6 ± 0.0	-7.7 ± 0.2	PHE170	-11.7 ± 0.2	2.2 ± 0.0	-0.6 ± 0.0	-10.2 ± 0.2
MET174	-4.9 ± 0.2	1.4 ± 0.1	-0.5 ± 0.0	-4.0 ± 0.2	MET174	-2.5 ± 0.1	1.9 ± 0.1	-0.3 ± 0.0	-0.9 ± 0.1
TRP177	-8.4 ± 0.2	2.8 ± 0.1	-0.5 ± 0.0	-6.1 ± 0.2	TRP177	-6.6 ± 0.1	1.6 ± 0.0	-0.5 ± 0.0	-5.5 ± 0.1
LYS178	-13.8 ± 0.6	18.9 ± 0.8	-0.2 ± 0.0	5.0 ± 0.4	LYS178	-1.2 ± 0.1	-1.8 ± 0.2	0.0 ± 0.0	-3.0 ± 0.1
GLU268	-8.2 ± 0.3	17.9 ± 0.6	-0.3 ± 0.0	9.3 ± 0.5	GLU268	-3.0 ± 0.4	16.3 ± 0.6	-0.2 ± 0.0	13.2 ± 0.4
GLU288	-0.3 ± 0.1	0.3 ± 0.0	0.0 ± 0.0	0.0 ± 0.1	GLU288	-0.4 ± 0.0	-0.3 ± 0.0	0.0 ± 0.0	-0.7 ± 0.0
PHE292	-2.2 ± 0.1	1.4 ± 0.1	-0.4 ± 0.0	-1.2 ± 0.1	PHE292	-3.3 ± 0.1	1.3 ± 0.1	-0.5 ± 0.0	-2.5 ± 0.1
PHE296	-7.1 ± 0.2	1.7 ± 0.1	-0.5 ± 0.0	-5.8 ± 0.2	PHE296	-6.1 ± 0.2	1.3 ± 0.1	-0.3 ± 0.0	-5.1 ± 0.2
ASP457	-19.7 ± 0.3	30.6 ± 0.7	-0.7 ± 0.0	10.3 ± 0.6	ASP457	-12.4 ± 0.4	25.0 ± 0.6	-0.6 ± 0.0	12.0 ± 0.6
PHE459	-14.6 ± 0.2	2.0 ± 0.0	-0.8 ± 0.0	-13.3 ± 0.2	PHE459	-12.3 ± 0.2	2.2 ± 0.1	-0.7 ± 0.0	-10.8 ± 0.2
GLU476	0.2 ± 0.3	1.9 ± 0.5	-0.3 ± 0.0	1.7 ± 0.4	GLU476	-0.1 ± 0.1	0.9 ± 0.1	0.0 ± 0.0	0.8 ± 0.1
NAD^+	-2.4 ± 0.1	6.1 ± 0.2	-0.1 ± 0.0	3.6 ± 0.2	NAD^+	-1.5 ± 0.1	2.3 ± 0.1	-0.0 ± 0.0	0.7 ± 0.1

[a]The residues with a contribution of > 1 kcal/mol are marked in blue and red for favorable and unfavorable interactions, respectively. Note that in the energy decomposition per residue by g_mmpbsa, the interaction energies are equally distributed on both interacting partners of the receptor residue and the inhibitor. For instance, the ΔE_{MM} part for NAD^+ in Table S4 is exactly half the values of Table S3.

Table S5. Occupancy of the Hydrogen Bonds Between Receptor and Inhibitor Observed in the Representative Binding Models in Figures 8 and S4

compound	residue	occupancy	compound	residue	occupancy
MSA-1	Gly270	0.31	**MSA-3**	Asn169	0.29
	Phe459	0.56		Cys302	< 0.01
	NAD^+	0.66		Asp457	0.81
OH-1	NAD^+	0.49	**OH-3**	Asp457	0.99
MSA-2	Glu288	0.83	**MSA-4**	Lys178	0.47
	Cys301	< 0.01	**OH-4**	Glu268	0.11
				Cys303	< 0.01

Table S6. Energy Decomposition (kJ/mol) for the Key Residues with a Large Contribution to the Binding of MSA-1 and OH-4 from Three Independent MD Simulations[a]

residue	#1			#2			#3		
	ΔE_{MM}	ΔG_{sol}	$\Delta E_{MM}+\Delta G_{sol}$	ΔE_{MM}	ΔG_{sol}	$\Delta E_{MM}+\Delta G_{sol}$	ΔE_{MM}	ΔG_{sol}	$\Delta E_{MM}+\Delta G_{sol}$
					MSA-1				
VAL120	-5.3 ± 0.1	-1.1 ± 0.1	-6.4 ± 0.1	-7.4 ± 0.1	-1.2 ± 0.0	-8.6 ± 0.1	-7.6 ± 0.1	-1.1 ± 0.0	-8.7 ± 0.1
ASP121	-1.3 ± 0.1	-0.7 ± 0.2	-2.0 ± 0.2	-1.6 ± 0.1	-1.1 ± 0.3	-2.7 ± 0.3	-1.0 ± 0.1	-3.1 ± 0.2	-4.1 ± 0.2
ASP123	0.3 ± 0.2	-2.7 ± 0.2	-2.4 ± 0.2	-2.0 ± 0.1	-1.6 ± 0.1	-3.7 ± 0.1	-1.4 ± 0.2	-1.9 ± 0.3	-3.3 ± 0.2
MET124	-6.6 ± 0.2	1.4 ± 0.1	-5.3 ± 0.1	-4.7 ± 0.1	1.3 ± 0.1	-3.4 ± 0.1	-4.1 ± 0.1	1.2 ± 0.1	-2.9 ± 0.1
LYS127	-2.1 ± 0.3	8.9 ± 0.7	6.8 ± 0.5	2.2 ± 0.1	1.2 ± 0.1	3.4 ± 0.1	0.8 ± 0.1	2.9 ± 0.4	3.7 ± 0.3
PHE170	-10.0 ± 0.1	1.5 ± 0.0	-8.5 ± 0.1	-4.6 ± 0.2	0.9 ± 0.1	-3.6 ± 0.1	-11.4 ± 0.2	1.5 ± 0.0	-9.9 ± 0.2
MET174	-5.4 ± 0.1	3.1 ± 0.1	-2.3 ± 0.1	-5.3 ± 0.3	1.7 ± 0.1	-3.5 ± 0.2	-4.8 ± 0.1	2.0 ± 0.1	-2.7 ± 0.1
TRP177	-4.9 ± 0.1	1.4 ± 0.1	-3.5 ± 0.1	-8.3 ± 0.2	2.1 ± 0.1	-6.2 ± 0.2	-5.4 ± 0.1	1.1 ± 0.1	-4.3 ± 0.1
LYS178	2.9 ± 0.0	-5.5 ± 0.2	-2.6 ± 0.2	-0.9 ± 0.9	3.4 ± 1.1	2.5 ± 0.5	2.6 ± 0.2	0.2 ± 0.4	2.8 ± 0.3
GLU268	-12.3 ± 0.1	13.7 ± 0.4	1.5 ± 0.3	-6.6 ± 0.9	15.4 ± 1.7	8.8 ± 0.9	-7.0 ± 0.3	11.2 ± 0.7	4.3 ± 0.6
GLU288	-0.8 ± 0.0	0.0 ± 0.0	-0.7 ± 0.0	-0.5 ± 0.0	-0.5 ± 0.0	-1.0 ± 0.0	-0.4 ± 0.0	-0.4 ± 0.0	-0.8 ± 0.0
PHE292	-0.4 ± 0.0	0.1 ± 0.0	-0.2 ± 0.0	-3.9 ± 0.1	0.8 ± 0.1	-3.1 ± 0.1	-4.0 ± 0.2	0.8 ± 0.1	-3.3 ± 0.2
PHE296	-6.7 ± 0.2	0.8 ± 0.0	-5.9 ± 0.2	-9.5 ± 0.1	2.0 ± 0.1	-7.5 ± 0.1	-7.4 ± 0.2	1.1 ± 0.1	-6.3 ± 0.2
ASP457	-15.0 ± 0.2	21.7 ± 0.4	6.7 ± 0.4	-8.4 ± 0.1	4.6 ± 0.3	-3.8 ± 0.3	-11.7 ± 0.2	25.7 ± 0.8	14.0 ± 0.7
PHE459	-16.2 ± 0.3	3.7 ± 0.1	-12.6 ± 0.2	-15.4 ± 0.2	2.3 ± 0.0	-13.1 ± 0.2	-10.5 ± 0.2	1.8 ± 0.1	-8.8 ± 0.2
GLU476	-2.3 ± 0.0	2.6 ± 0.1	0.3 ± 0.1	-2.5 ± 0.3	1.8 ± 0.6	-0.7 ± 0.5	-2.0 ± 0.1	0.3 ± 0.1	-1.7 ± 0.1
NAD+	-9.5 ± 0.2	12.1 ± 0.2	2.6 ± 0.2	-5.0 ± 0.2	8.0 ± 0.4	3.0 ± 0.2	-13.9 ± 0.2	11.6 ± 0.2	-2.2 ± 0.3
ΔE_{bind}		-132.3 ± 7.6			-140.8 ± 10.5			-127. 8 ± 3.3	
					OH-4				
VAL120	-4.1 ± 0.1	-0.5 ± 0.0	-4.6 ± 0.1	-4.6 ± 0.1	-1.2 ± 0.0	-5.8 ± 0.1	-4.2 ± 0.1	-0.4 ± 0.0	-4.5 ± 0.1
ASP121	-1.2 ± 0.1	-2.1 ± 0.2	-3.4 ± 0.1	-0.1 ± 0.1	-1.1 ± 0.2	-1.2 ± 0.2	-1.7 ± 0.1	1.1 ± 0.2	-0.6 ± 0.2

ASP123	-1.4 ± 0.1	-1.1 ± 0.1	-2.5 ± 0.1	-0.1 ± 0.1	-2.0 ± 0.1	-2.0 ± 0.1	-2.1 ± 0.1	-0.3 ± 0.1	-2.4 ± 0.0
MET124	-4.6 ± 0.1	1.4 ± 0.1	-3.1 ± 0.1	-3.2 ± 0.1	1.3 ± 0.1	-1.9 ± 0.1	-4.4 ± 0.1	1.6 ± 0.1	-2.8 ± 0.1
LYS127	1.0 ± 0.1	1.2 ± 0.1	2.1 ± 0.1	-0.2 ± 0.1	1.8 ± 0.1	1.5 ± 0.1	1.8 ± 0.1	0.3 ± 0.0	2.1 ± 0.1
PHE170	-11.7 ± 0.2	1.6 ± 0.0	-10.2 ± 0.2	-7.5 ± 0.2	1.7 ± 0.1	-5.8 ± 0.1	-11.5 ± 0.2	1.7 ± 0.0	-9.8 ± 0.2
MET174	-2.5 ± 0.1	1.6 ± 0.1	-0.9 ± 0.1	-5.2 ± 0.1	1.1 ± 0.1	-4.1 ± 0.1	-3.2 ± 0.1	1.4 ± 0.1	-1.8 ± 0.1
TRP177	-6.6 ± 0.1	1.1 ± 0.0	-5.5 ± 0.1	-6.2 ± 0.1	1.4 ± 0.1	-4.7 ± 0.1	-6.7 ± 0.1	1.5 ± 0.0	-5.2 ± 0.1
LYS178	-1.2 ± 0.1	-1.8 ± 0.2	-3.0 ± 0.1	2.3 ± 0.0	-2.1 ± 0.2	0.3 ± 0.2	2.9 ± 0.0	-2.4 ± 0.2	0.5 ± 0.2
GLU268	-3.0 ± 0.4	16.2 ± 0.6	13.2 ± 0.4	-6.2 ± 0.4	9.1 ± 0.8	2.9 ± 0.4	-4.8 ± 0.1	8.4 ± 0.3	3.6 ± 0.3
GLU288	-0.4 ± 0.0	-0.3 ± 0.0	-0.7 ± 0.0	-0.7 ± 0.1	-0.3 ± 0.0	-1.0 ± 0.0	0.3 ± 0.0	-0.7 ± 0.0	-0.4 ± 0.0
PHE292	-3.3 ± 0.1	0.9 ± 0.1	-2.5 ± 0.1	-1.2 ± 0.1	0.1 ± 0.1	-1.0 ± 0.1	-3.4 ± 0.1	-0.2 ± 0.1	-3.6 ± 0.1
PHE296	-6.1 ± 0.2	1.0 ± 0.1	-5.1 ± 0.2	-7.7 ± 0.2	0.8 ± 0.1	-6.9 ± 0.2	-5.0 ± 0.1	0.5 ± 0.0	-4.5 ± 0.1
ASP457	-12.4 ± 0.4	24.3 ± 0.6	12.0 ± 0.6	-13.2 ± 0.2	19.5 ± 0.4	6.3 ± 0.4	-10.2 ± 0.3	26.1 ± 0.5	15.9 ± 0.5
PHE459	-12.3 ± 0.2	1.5 ± 0.1	-10.8 ± 0.2	-12.1 ± 0.2	1.6 ± 0.0	-10.5 ± 0.2	-12.1 ± 0.2	1.5 ± 0.1	-10.6 ± 0.2
GLU476	-0.1 ± 0.1	0.9 ± 0.1	0.8 ± 0.1	-1.8 ± 0.1	0.9 ± 0.1	-0.9 ± 0.1	-2.2 ± 0.1	1.1 ± 0.2	-1.1 ± 0.1
NAD^+	-1.5 ± 0.1	2.3 ± 0.1	0.7 ± 0.1	-4.4 ± 0.1	8.4 ± 0.2	4.0 ± 0.2	-1.3 ± 0.0	3.0 ± 0.2	1.7 ± 0.2
		-88.1 ± 5.6			-85.4 ± 4.6			-90.2 ± 2.0	

[a]Three replicas (#1–#3) for the MM-PBSA analysis were based on independent MD trajectories with different initial velocities. The results for #1 are shown in the main text. The total binding energies for the inhibitors (ΔE_{bind}) from the three runs are given as well. The values with a contribution of > 1 kcal/mol are marked in blue and red for favorable and unfavorable interactions, respectively.

Table S7. Configurational Entropy (*S*, J/mol/K) and Entropy Changes (-*T*Δ*S*, kJ/mol) of the Inhibitors Estimated with quasi-harmonic approximation[a]

compound	quasiharmonic approximation			Schlitter formula		
	S (bound)	*S* (free)	-*T*Δ*S*	*S* (bound)	*S* (free)	-*T*Δ*S*
MSA-1	245.2	598.0	105.2	289.7	642.7	105.3
OH-1	211.5	401.8	56.7	251.1	443.0	57.2
MSA-2	618.5	1136.0	154.3	676.6	1184.5	151.4
OH-2	578.5	900.0	95.8	632.5	947.9	94.0
MSA-3	348.9	677.6	98.0	398.1	726.2	97.8
OH-3	204.0	465.1	77.8	247.3	511.3	78.7
MSA-4	270.6	497.8	67.8	305.7	530.4	67.0
OH-4	164.7	275.6	33.1	194.4	305.9	33.2

[a]Two approaches of the quasi-harmonic approximation[1] and Schlitter formula[2] were used to computed the configurational entropy. The entropy change (Δ*S*) was computed as the difference between the bound and unbound (free) states.

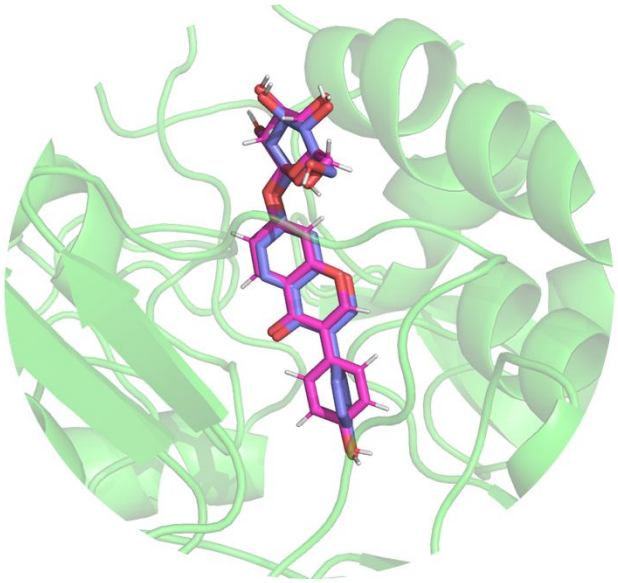

Figure S1. Comparison of the docking pose (colored in magenta) with the crystal structure (in blue) for the inhibitor **OH-3** (daidzin) using the Autodock Vina software

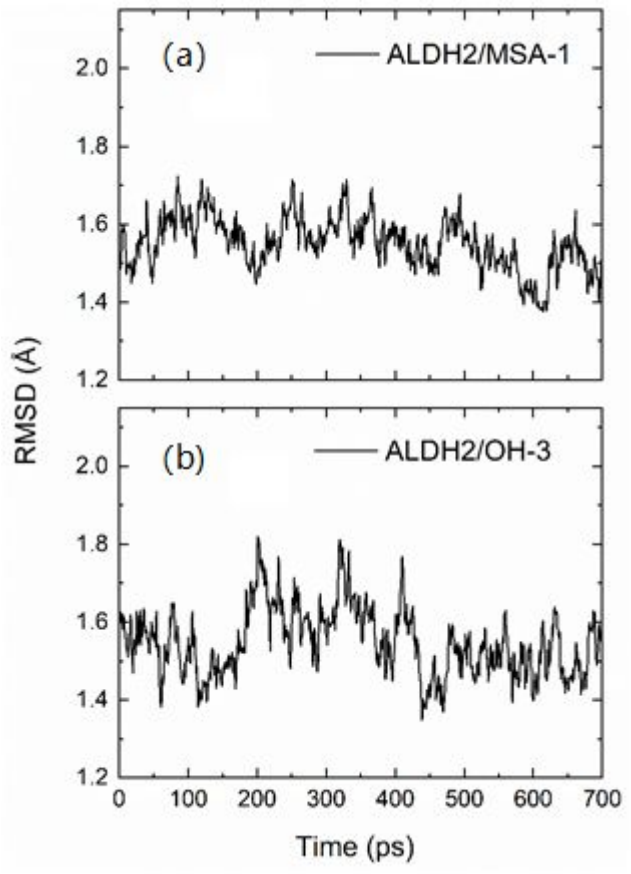

Figure S2. Root-mean-square deviations (RMSDs) of ALDH2 backbone from crystal structure when pulling the inhibitors of **MSA-1** (a) and **OH-3** (b) away from the binding tunnel of ALDH2.

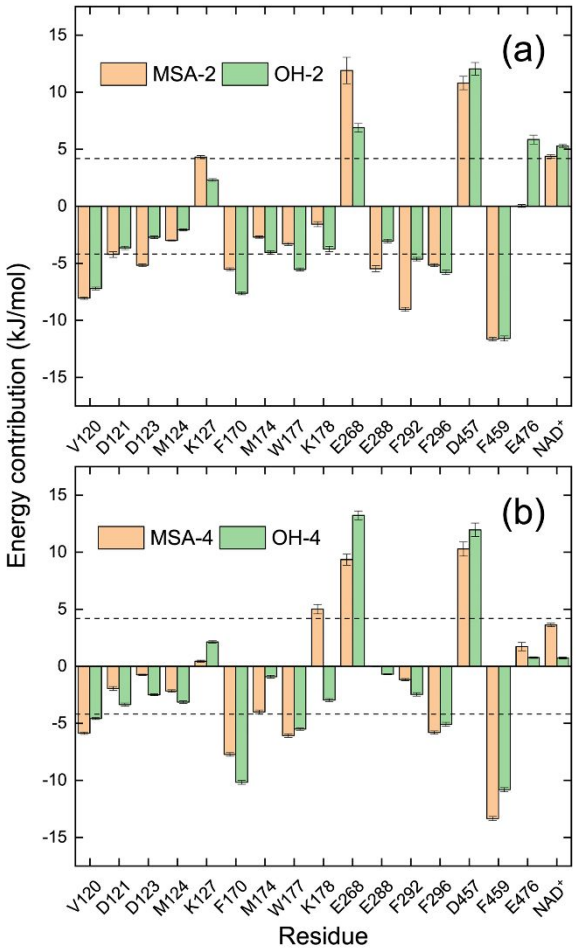

Figure S3. Energy contribution per residue to the binding of ALDH2 with the inhibitors of **MSA-2** and **OH-2** (a) as well as **MSA-4** and **OH-4** (b). The shown residues have a contribution of ≥ 1 kcal/mol to the binding with ALDH2 for at least one of the eight inhibitors tested. Dashed lines indicate a value of 1 kcal/mol. The cofactor NAD^+ is regarded as a residue of the receptor.

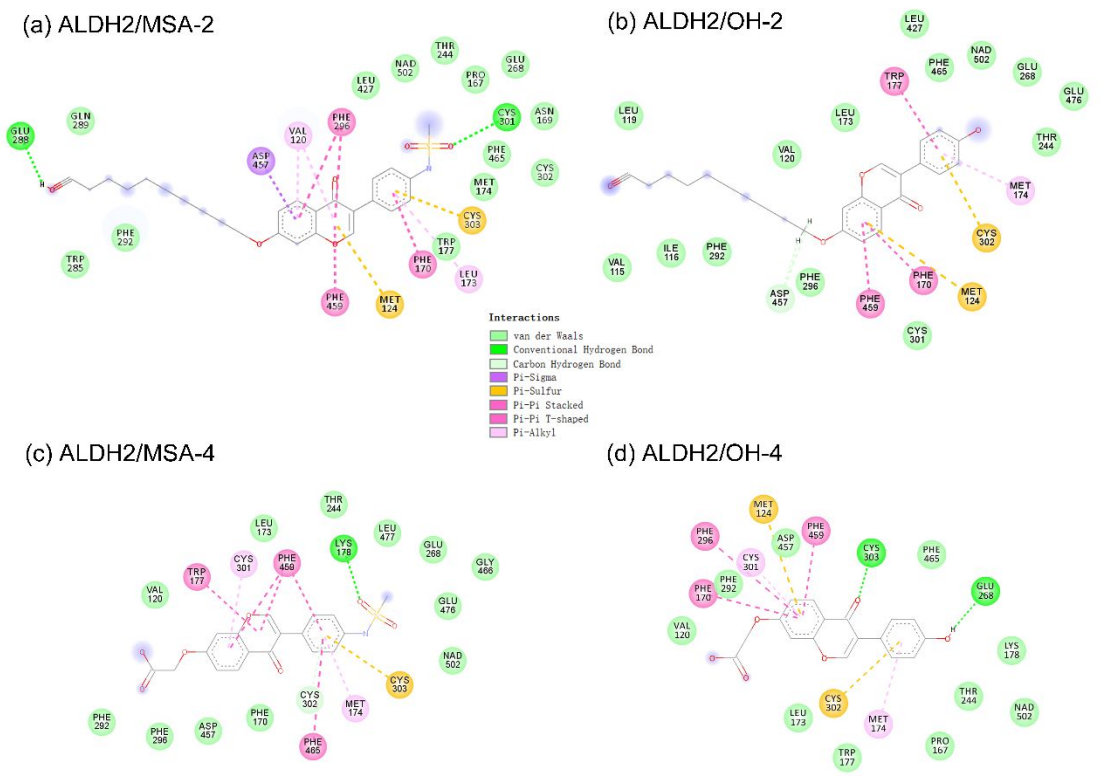

Figure S4. 2D diagrams of receptor−inhibitor interactions for ALDH2 complexes with **MSA-2** (a), **OH-2** (b), **MSA-4** (c), and **OH-4** (d). ALDH2 has 500 amino acids and the residue IDs for the inhibitor and NAD^+ are 501 and 502, respectively, in our simulation. The figures were generated by the Biovia Discovery studio visualizer software and the complexes are representative structures clustered from the last 10 ns simulations.

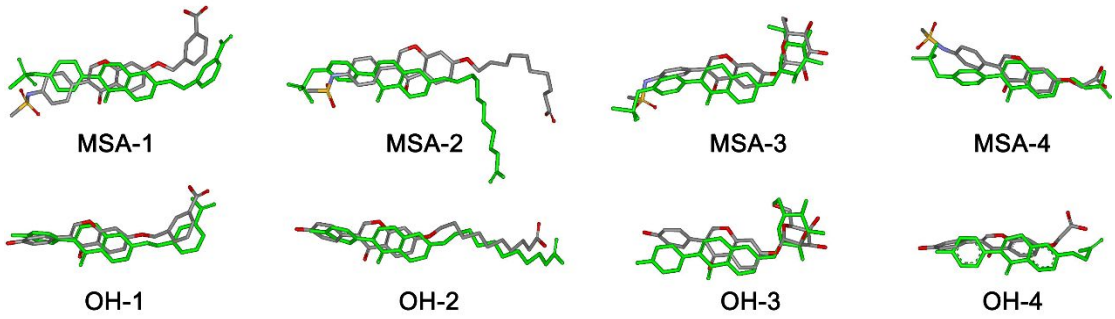

Figure S5. Binding poses of the inhibitors with ALDH2 relative to the crystal structure of ALDH2/**OH-3** (PDB 2VLE). The isoflavone skeleton of the inhibitors with green sticks are aligned with the crystal position of **OH-3**. The inhibitors colored by element are the representative binding poses from 30 ns MD simulations via aligning the protein backbone of ALDH2 with the chain A of PDB 2VLE.

References

(1) Andricioaei, I.; Karplus, M. On the Calculation of Entropy from Covariance Matrices of the Atomic Fluctuations. *J. Chem. Phys.* **2001**, *115*, 6289-6292.

(2) Schlitter, J. Estimation of Absolute and Relative Entropies of Macromolecules Using the Covariance Matrix. *Chem. Phys. Lett.* **1993**, *215*, 617-621.